

Fabrication and Mechanical Characterization of PLA/PCL-MCC Bio-composite Filaments for FDM 4D Printing

Octarina Adiati Juniasih^{1*}, *Fahmi Mubarok*¹, and *Alvin Widjaya*²

¹Department of Mechanical Engineering, Faculty of Industrial Technology and Systems Engineering, Institut Teknologi Sepuluh Nopember, 60111, Surabaya, Indonesia.

²Faculty of Georesources and Materials Engineering, RWTH Aachen University, Aachen 52064, Germany.

Abstract. Polylactic Acid (PLA) has been gaining potential for 4D printing application. 4D printing is an emerging technology where 3D printed objects are designed to change shape in response to external stimuli. This innovation has potential applications in smart materials, self-healing structures, and adaptive devices for wide range of applications. However, the limitations of PLA such as brittleness and shape-memory properties. To address this issue, the Polycaprolactone (PCL) is incorporated in this study. this study investigates PLA/PCL-MCC bio-composite filaments with tailored properties for 4D printing. PLA and Polycaprolactone (PCL) were blended in ratios of 90/10, 80/20, and 70/30, with 1% Microcrystalline Cellulose (MCC) as a reinforcing filler. Mechanical properties, including yield strength, ultimate tensile strength, Young's modulus, and elongation at break, were evaluated through tensile testing. Fourier-transform infrared spectroscopy (FTIR) was also conducted to examine the chemical composition and structure. The results revealed that the 90:10 PLA/PCL composition exhibited superior mechanical properties, achieving the highest ultimate tensile strength of 40.18 MPa. This study provides valuable insight into the incorporation of PCL and MCC in PLA-based composites, highlighting their potential for use in 3D and 4D printing applications.

1 Introduction

The additive manufacturing (AM) is an advance manufacturing technology which also popular as 3D printing technology [1]. It employed as a layer-by-layer production technique that allows complex geometries to be fabricated with minimal material waste and does not require additional machining process. Its applications span across various industries including biomedical engineering, aerospace, and automotive sectors [2, 3]. Over the past decade, AM has evolved into a more advanced concept known as 4D printing, where time integrated as the fourth dimension. In this recent concept, the 3D printed objects are

*Corresponding author: octarina.oct@gmail.com

programmed to have the ability to transform their shape to the desirable geometries in response to the external stimulus. This innovation offers significant potential for smart materials in a variety of applications, including self-healing structures, adaptive devices, and intelligent robotics. In the biomedical applications itself, 4D printing is potential for multiple applications including medical assistive device or even drugs delivery systems [4].

The development of 4D printing technology depends on several key factors, including the choice of materials and the type of external stimuli applied [5]. A crucial requirement for 4D printing is the use of shape-memory materials, such as shape-memory polymers, alloys, composites, hydrogels, and others. Among the various materials utilized in 3D and 4D printing, Polylactic Acid (PLA) has gained significant attention due to its biodegradability, renewable source, and excellent printability [6]. PLA is derived from natural sources like corn starch or sugarcane which aligns with the demand of eco-friendly manufacturing technologies. Additionally, since PLA is sourced from agricultural products, it becomes potential for biomedical applications. However, despite its advantages, PLA's brittleness, low impact strength, and shape-memory properties present challenges when it comes to its use in more functional 4D printing applications, particularly where durability and flexibility are required. PLA exhibits mechanical properties similar to bone and with a relatively good shape memory characteristics, its brittleness and low elongation capacity limit its use in tissue engineering applications [7]. When combined with PLA, PCL enhances the flexibility and thermal responsiveness of the material, making the resulting blend more suitable for shape-morphing applications [8]. Additionally, PCL has a relatively low glass transition temperature (T_g) of around -60°C , which can possibly lower the overall T_g of the PLA/PCL blend, thus improving its functional versatility. However, while the addition of PCL improves flexibility, it also tends to reduce the mechanical strength of the composite.

To counterbalance this reduction in strength, the incorporation of natural fillers has been explored to reinforce the mechanical properties of the composite. One such filler is Microcrystalline Cellulose (MCC), which is derived by hydrolysing cellulose into micro-sized crystallites [9, 10]. MCC is highly valued for its renewable origin, high aspect ratio, and robust hydrogen bonding capability, making it an effective reinforcement agent in biopolymer matrices. Tomec et al. [11] incorporated 1, 3, and 5 wt% of MCC into Wood-PLA, and found that the addition of 1 wt% MCC had the most significant positive effect on the tensile strength of the composite. This suggests that even a small amount of MCC can significantly enhance composite performance, offering a sustainable approach to strengthening PLA/PCL biopolymers composite.

This research aims to fabricate and mechanically characterize PLA/PCL-MCC biocomposite filaments with tailored properties for 4D printing. The objective is to optimize the blend ratios of PLA and PCL while maintaining a fixed 1% MCC content, and to evaluate the resulting materials through Fourier-transform infrared spectroscopy (FTIR) and mechanical tensile testing as the first step in characterize the compatibility of the filament for printing application. The goal is to develop a sustainable, smart material filament that further combines printability, biodegradability, and stimuli-responsive behaviour, contributing to the advancement of materials for next-generation 4D printing technologies.

2 Introduction

2.1 Material Preparation

In this study, PLA pellets (Revode 110) sourced from Hisun, China, with a density of $1.25 \pm 0.05 \text{ g/cm}^3$ and a melting temperature range of $155\text{--}170^\circ\text{C}$, were used. PCL pellets, also procured from China. Microcrystalline Cellulose (MCC) powder, obtained from MERCK,

has a density of 1.5 g/cm³ at 20°C. To ensure optimal processing conditions, both the PLA and PCL granules were dried in a vacuum oven at a low temperature of 40°C for 24 hours to remove any moisture content.

2.2 Mixing Process

The dried PLA and PCL pellets are then weighed and mixed in various composition ratios of 90/10, 80/20, 70/30. The PLA/PCL pellets are then ground and mixed using a high-speed grinding mixer (see. Fig. 1). Subsequently, the PLA/PCL blend and 1% MCC powders are combined in a rotary mixing container (without milling balls) and processed at 150 rpm for 1 hour to ensure thorough mixing. Additionally, 1 wt% of stearic acid is added prior to mixing MCC to serve as a lubricant during the extrusion process. The detail compositions were listed on Table 1.

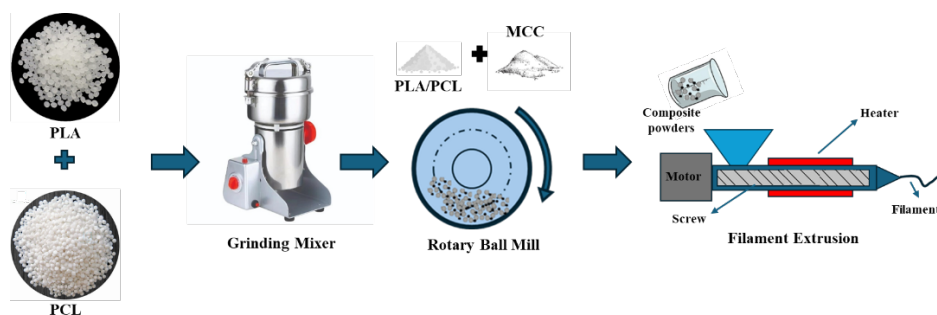


Fig. 1. Schematic diagram of the powder mixing process leading to extrusion.

Table 1. Blending Composition and Labelling

Name	Weight Percent of PLA: PCL: MCC (wt%)	PLA (gr)	PCL (gr)	MCC (gr)
PLA70/PCL30-MCC	69.1:9.9:1	70	30	1.01
PLA80/PCL20-MCC	79.2:19.8:1	80	20	1.01
PLA90/PCL10-MCC	89.1:9.9:1	90	10	1.01

2.3 Extrusion Process

The blended composites are extruded using a single-screw filament extruder. The dried and well-mixed powders are loaded into the hopper of a single-screw extruder (Wellzoom, Shenzhen Mistar Technology Co., Ltd, China) extruded into 1.75 mm diameter filaments at a rotor speed of 20 rpm. The barrel temperatures, from hopper to die, are set within the range of 170°C.

2.4 Filament Characterization

2.4.1 Filament Diameter Uniformity

Filament diameter was measured at 1 cm intervals along a 30 cm length using a digital calliper (± 0.01 mm) to assess uniformity. The average diameter and standard deviation were calculated and compared to 1.75 mm FDM filaments. Maintaining uniform diameter is essential to ensure consistent extrusion and mechanical reliability during 4D printing. The Coefficient of Variation (CV) was then calculated to quantify the relative variability in diameter across the measured filament length. The CV is given by the formula:

$$CV = \frac{\sigma}{\mu} \times 100 \quad (1)$$

Where σ is the standard deviation of the filament diameter, and μ is the mean diameter. A lower CV value indicates greater uniformity, which is crucial for ensuring stable 3D printing performance. The CV of the filament was assessed to ensure that its diameter uniformity to ensure a better extrusion result during the printing process.

2.4.2 FTIR

Fourier Transform Infrared Spectroscopy (FTIR) will be used to analyse the chemical composition and interactions conducted on the synthesized filaments. By examining the peaks in the resulting spectra, specific chemical bonds and functional groups present in the composites can be identified. This analysis will provide valuable insights into the molecular structure of the materials, revealing any interactions or chemical changes occurring between the PLA, PCL, and MCC components, and helping to further understand the behaviour of the composites in the 4D printing process.

2.4.3 Tensile Test

The mechanical properties of the extruded filament were examined using tensile testing. The setup involved the use of the ESM301L motorized test stand, which was used for various mechanical test, including tensile, compression, break, and cycling. The tensile testing conducted ASTM C1557 [12] single fibre filament testing standard with a speed of 10mm/min and a gauge length of 80 mm. The illustration of the tensile specimen shown on Figure 2. The tests were performed at a constant extension rate of 10 mm per minute until specimen rupture under standardized conditions of 23°C air temperature and 50% relative humidity. Each material was tested with at least three repetitions to ensure statistical reliability of the data. The parameters and condition detailed on Table 2.

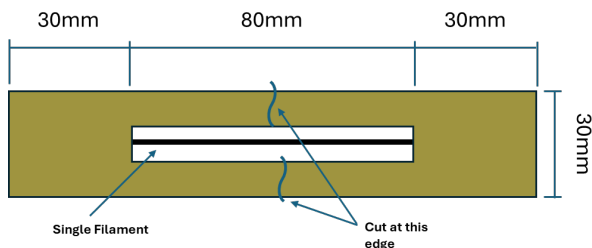


Fig. 2. Tensile test specimen for single fibre based on ASTM C1557.

Table 2. Tensile Testing Parameters

Parameters	Specification
Tensile Testing Machine	ESM301L Motorized Test Stand
Load Cell Capacity	1.5 kN
Initial Load	0.1 MPa
Gauge Length	80 mm
Testing Environment	23°C Air Temperature, 50% Relative Humidity
Testing Speed	10 mm/min

3 Result and Discussion

3.1 Filament Uniformity

The fabricated filaments with three composition variations were shown on the Figure 3. It illustrates the fabricated filaments with three composition variations which are PLA90/PCL10-MCC, PLA80/PCL20-MCC, and PLA70/PCL30-MCC, compared to a standard PLA filament (the red filament). The average or mean diameters of the filaments were measured, with PLA90/PCL10-MCC has a diameter of 1.73mm, PLA80/PCL20-MCC at 1.63mm, and PLA70/PCL30-MCC at 1.60mm. These values are generally close to the standard filament diameter of 1.75mm, which is widely used in FDM 3D printing. To assess the uniformity, the CV of the filament diameter standard deviation was calculated, with displayed on the bar chart (see Fig. 4). The figure illustrates the mean diameter in blue, the standard deviation in orange, and the coefficient of variation (CV) represented by green bars. Typically, a CV below 10% is considered good, while values under 5% are regarded as very good. A CV below 1% indicates outstanding consistency and minimal variation among the samples, reflecting the high precision of the fabrication process [13].

The PLA90/PCL10-MCC blend exhibited the lowest CV of 0.99%, indicating excellent diameter uniformity with less than 1% CV. In contrast, the PLA80/PCL20-MCC blend showed a moderate CV of 3.29%, suggesting a moderate increase in variability compared to the PLA90/PCL10-MCC blend. The PLA70/PCL30-MCC blend displayed the highest CV of 5.60%, indicating significant diameter variability. This result is consistent with PLA's rheological behavior. PLA, being a semi-crystalline polymer with a higher melting point and greater viscosity, maintains a stable extrusion process with less shrinkage during cooling compared to PCL. PLA's rigid structure enhances its dimensional stability, contributing to less variability in filament diameter during the production process. Meanwhile since PCL considered amorphous an amorphous polymer with a lower melting point and reduced viscosity, introduces greater flexibility to the filament. This flexibility, combined with PCL's higher thermal expansion, leads to increased variability during the extrusion and cooling processes. The results demonstrate that PLA90/PCL10-MCC offers the best uniformity in filament diameter and closest to the diameter of commercially available PLA.

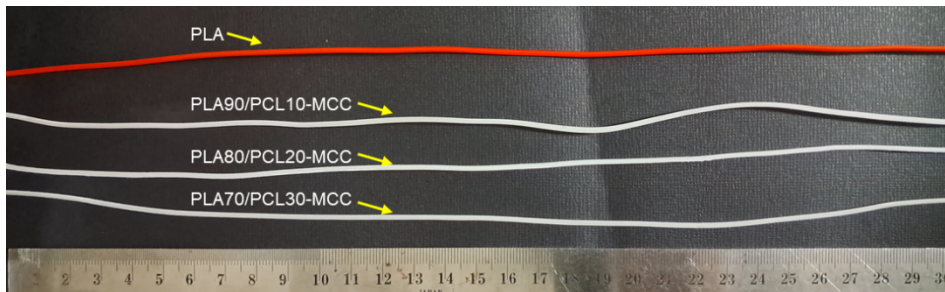


Fig. 3. PLA/PCL-MCC filament samples comparisons

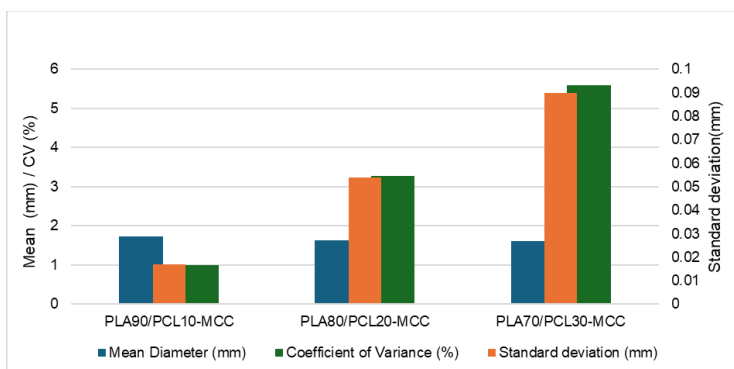


Fig. 4. Filament diameter measurements and Coefficient of Variation (CV) for different PLA/PCL-MCC blends.

3.2 FTIR

Fourier Transform Infrared (FTIR) spectroscopy was conducted to identify the functional groups and assess potential intermolecular interactions in the bio-composite filaments. Figure 5 presents the FTIR spectra of three different blend compositions: PLA90/PCL10-MCC, PLA80/PCL20-MCC, and PLA70/PCL30-MCC.

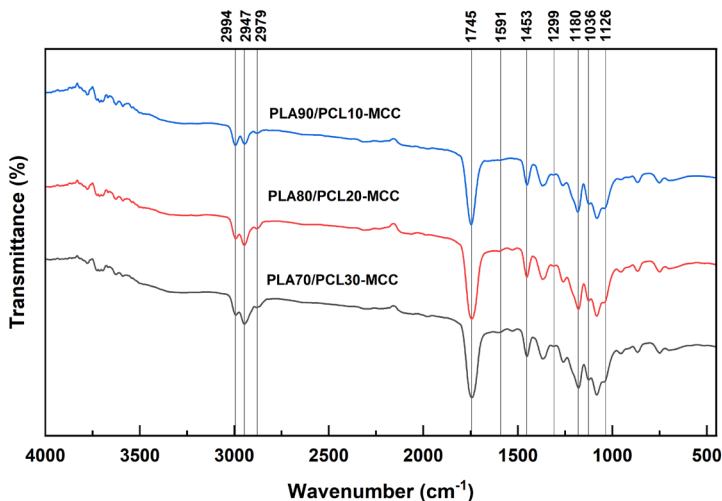


Fig. 4. FTIR spectra of the fabricated PLA/PCL-MCC blends

The results show clear differences in the spectra as the ratio of PLA to PCL changes. In the PLA90/PCL10-MCC blend, the spectra reveal prominent peaks at 2994 cm⁻¹ and 2977 cm⁻¹, corresponding to the C-H stretching vibrations of PLA, indicating that PLA predominates in this composite. The overall transmittance in this region is relatively high, reflecting the higher PLA content and minimal contributions from PCL and MCC. As the PCL content increases in the PLA80/PCL20-MCC blend, the spectra show additional peaks around 1745 cm⁻¹, attributed to the ester C=O stretching vibration characteristic of PCL, indicating the increased presence of PCL in the composite. This is further supported by the appearance of peaks at 1591 cm⁻¹, which correspond to C-H bending vibrations, suggesting stronger interaction between PLA and PCL. The presence of MCC is also confirmed by the peaks observed in the lower wavenumber region, such as 1299 cm⁻¹, 1259 cm⁻¹, 1088 cm⁻¹, and 1126 cm⁻¹, which are characteristic of cellulose-based materials.

In the PLA70/PCL30-MCC blend, the spectrum exhibits an even greater intensity of the 1745 cm⁻¹ peak, indicating a dominant presence of PCL. The peaks at 1591 cm⁻¹ and 1453 cm⁻¹, associated with C-H bending and deformation vibrations, become more pronounced, further emphasizing the increase in PCL content. Additionally, the peaks corresponding to MCC, such as those at 1299 cm⁻¹, 1259 cm⁻¹, 1088 cm⁻¹, and 1126 cm⁻¹, increase in intensity, confirming the incorporation of MCC into the composite. These observations suggest that as the PCL content increases, there is a corresponding shift in the functional group distribution, with a greater influence of PCL and MCC in the composite material. The analysis clearly indicates that adjusting the PLA/PCL ratio can significantly impact the chemical structure and properties of the composite, which is important for tailoring these materials for various applications, particularly in biodegradable and sustainable material design.

3.3 Tensile

The tensile test was performed by testing three samples per composition as repetition. The testing machine recorded the time and applied load, which were subsequently converted into stress-strain curves. Figures 6 display the stress-strain curves of the tensile test result, with detailed tensile property values summarized in Table 3.

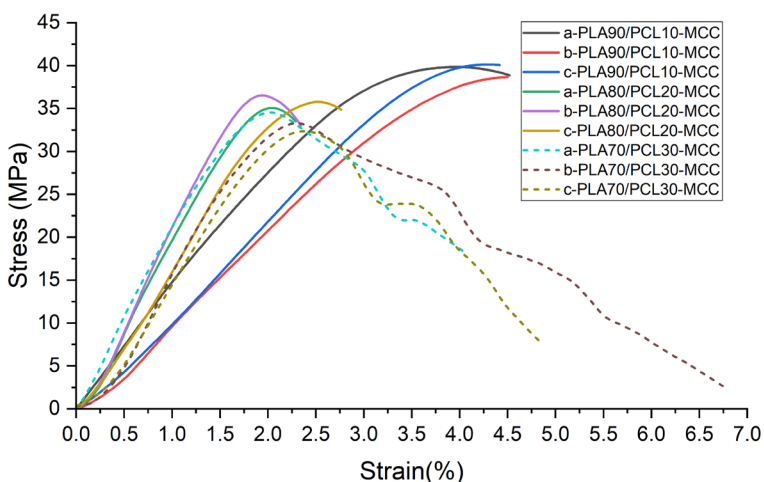


Fig. 6. Illustrate the stress–strain behaviour of PLA/PCL-MCC filaments with three different PLA/PCL composition ratio (90/10, 80/20, and 70/30), each containing 1 wt% microcrystalline cellulose (MCC). For each composition, three specimens were tested to evaluate the repeatability and variation in mechanical response. Overall, the specimens within each composition group exhibited consistent stress–strain behaviour, indicating good repeatability of the tensile measurements. The general trend observed indicates that as the PCL content increases, the tensile strength decreases, while the ductility, represented by strain at break, increases slightly. The PLA90/PCL10-MCC specimens (black, red, and blue lines) exhibited the highest tensile strength among the tested compositions, with sample c reaching a peak value of 40.18 MPa and an average ultimate tensile strength (UTS) of 39.65 ± 0.73 MPa. These specimens also showed relatively low elongation at break, indicating a more brittle behaviour. This is consistent with the inherent stiffness and high modulus of PLA, which dominates the mechanical response in this high-PLA-content formulation, compared to the more ductile nature of PCL.

In contrast, the PLA70/PCL30-MCC specimens (dashed lines graph) demonstrated the highest elongation at break among all compositions, indicating improved ductility. While the average UTS decreased to 33.40 ± 1.08 MPa, the stress–strain curves exhibited a more gradual post-yield response and extended strain values, particularly in sample a, which reached a strain of over 6%. This possibly occurs due to the possibly due to differences in MCC dispersion as the ratio of the PCL increased. This behaviour reflects the increasing influence of PCL at higher concentrations, which contributes to enhanced flexibility of the filament.

The intermediate composition, PLA80/PCL20-MCC presents a balanced mechanical response, with moderate strength and strain at break. This group shows less variation among replicates, which may indicate more stable interfacial bonding and uniformity. The results of the highest ultimate tensile test 36.56 MPa with mean of 35.56 ± 0.87 MPa. Interestingly, the PLA80/PCL20-MCC specimens exhibited the lowest elongation at break ($2.43 \pm 0.19\%$), despite having an intermediate PCL content. This unexpected result may be attributed to poor interfacial adhesion between PLA and PCL at this ratio, or to MCC agglomeration disrupting the PCL phase continuity. Additionally, the higher Young’s Modulus of this group suggests a more brittle behaviour, possibly due to localized stress concentrations or limited polymer chain mobility. These factors may have led to premature failure under tensile loading.

Table 3. Table of mechanical properties of each bio-composite filament variations.

Composition	Ultimate Tensile Strength (MPa)	Youngs Modulus (GPa)	Elongation at break (%)
PLA90/PCL10-MCC	39.95	1.39	4.52
	38.81	1.23	4.12
	40.18	1.14	4.42
PLA80/PCL20-MCC	35.06	2.13	2.29
	35.56	2.33	2.33
	35.06	1.89	2.66
	34.52	2.01	4.03

PLA70/PCL30-MCC	33.32	1.95	6.74
	32.36	1.74	4.87

Overall, the incorporation of MCC appears to reinforce the PLA/PCL matrix, contributing to increased stiffness while also introducing variability depending on composition and dispersion quality. A more detailed summary of tensile properties is provided in Table 5. The data reveals a clear trend in how the material's mechanical performance changes with varying compositions of PLA and PCL. As the PCL content increases in the composite, both the yield strength and ultimate tensile strength decrease, while the elongation at break increases, demonstrating a shift from strength to flexibility.

The tensile test results of the PLA/PCL-MCC bio-composite filaments indicate that PLA90/PCL10-MCC offers the most balanced and optimal mechanical performance for filament-based 3D and 4D printing applications. This composition exhibited the highest ultimate tensile strength and a moderate elongation at break ($4.35 \pm 0.20\%$), along with a relatively low Young's modulus (1.25 ± 0.13 GPa). The lower stiffness suggests that the filament maintains a degree of flexibility while remaining structurally robust, which is beneficial in additive manufacturing where both strength and controlled compliance are required. The moderate modulus also allows the material to absorb mechanical stresses during extrusion and layer deposition without fracturing, improving print reliability. In comparison, PLA70/PCL30-MCC exhibited higher ductility and toughness but lower strength, making it better suited for non-structural or highly flexible prints. A high ductility filament could lead into poor dimensional stability during the printing process [14]. Meanwhile, PLA80/PCL20-MCC had the highest Young's modulus (2.12 ± 0.22 GPa), indicating increased stiffness, but also showed the lowest elongation. This minimal elongation suggests that the filament is comparatively more brittle than the other compositions, potentially leading to a higher risk of mechanical failure or breakage during extrusion and printing. Overall, PLA90/PCL10-MCC's combination of high strength, sufficient elongation, and moderate stiffness makes it the potential candidate for functional and responsive 4D printing filaments.

4 Conclusion

The fabrication of PLA/PCL/MCC bio-composite filaments with varying compositions demonstrated the feasibility of mechanical properties through compositional variations. Among all variants, PLA90/PCL10-MCC exhibited the highest tensile strength and stiffness, along with excellent dimensional consistency (1.73 mm diameter, CV < 1%), closely resembling the commercial PLA filament standards. FTIR analysis confirmed enhanced molecular interactions with increased PCL content, supporting the observed changes in mechanical behaviour. A clear trade-off was identified where higher PLA content improved the tensile strength, while higher PCL content enhanced flexibility at the cost of tensile performance. These findings suggest that by tuning the PLA/PCL ratio, the properties of the filament can be optimized for specific applications. In this analysis, PLA90/PCL10-MCC emerged as the most balanced and promising formulation, offering a combination of high mechanical strength and excellent diameter uniformity, which enhances its printability and suitability for sustainable 3D printing and further 4D printing applications.

Acknowledgements: The authors gratefully acknowledge financial support provided by the Department of Mechanical Engineering, Institut Teknologi Sepuluh Nopember Batch II year 2025. The author also acknowledges the support of Energy and Environmental Laboratory, Institut Teknologi Sepuluh Nopember for their characterization and testing services.

References

1. M. Bodaghi and A. Zolfagharian, 4D printing principles and manufacturing. *Smart Materials in Additive Manufacturing*, **1**, 1–17 (2022) [doi: 10.1016/B978-0-12-824082-3.00014-3](https://doi.org/10.1016/B978-0-12-824082-3.00014-3)
2. Y. S. Alshebly, M. Nafea, M. S. Mohamed Ali, and H. A. F. Almurib, Review on recent advances in 4D printing of shape memory polymers. *Eur. Polym. J.* **159**, 110708 (2021) [doi: 10.1016/j.eurpolymj.2021.110708](https://doi.org/10.1016/j.eurpolymj.2021.110708).
3. Y. S. Alshebly et al., Bioinspired Pattern-Driven Single-Material 4D Printing for Self-Morphing Actuators. *Sustainability* **16**, 10141 (2022) [doi: 10.3390/su141610141](https://doi.org/10.3390/su141610141)
4. M. G. Sahini, Poly(lactic acid) (PLA)-based materials: a review on the synthesis and drug delivery applications. *Emergent Mater.* **6**, 1461–1479 (2023) [doi: 10.1007/s42247-023-00551-7](https://doi.org/10.1007/s42247-023-00551-7)
5. K. Saptaji et al., Enhancing shape-recovery ratio of 4D printed poly(lactic acid) (PLA) structures through processing parameter optimization. *Prog. Addit. Manuf.*, (2023) [doi: 10.1007/s40964-023-00551-3](https://doi.org/10.1007/s40964-023-00551-3)
6. M. Barletta, A. Gisario, and M. Mehrpouya, 4D printing of shape memory poly(lactic acid) (PLA) components: Investigating the role of the operational parameters in fused deposition modelling (FDM). *J. Manuf. Process.* **61**, 473–480 (2021) [doi: 10.1016/j.jmapro.2020.11.036](https://doi.org/10.1016/j.jmapro.2020.11.036)
7. M. Eryildiz, A. Karakus, and M. Altan Eksi, Development and Characterization of PLA/PCL Blend Filaments and 3D Printed Scaffolds. *J. Mater. Eng. Perform.*, (2024) [doi: 10.1007/s11665-024-10247-6](https://doi.org/10.1007/s11665-024-10247-6)
8. S. Ma et al., 4D printing of PLA/PCL shape memory composites with controllable sequential deformation. *Bio-Des. Manuf.* **4**, 867–878 (2021) [doi: 10.1007/s42242-021-00151-6](https://doi.org/10.1007/s42242-021-00151-6)
9. F. Fahma, Potential Application of Nanocellulose for Filaments Production: A Review. (2020). [DOI:10.22052/JNS.2020.03.011](https://doi.org/10.22052/JNS.2020.03.011)
10. S. Mohan Bhasney, A. Kumar, and V. Katiyar, Microcrystalline cellulose, poly(lactic acid) and polypropylene biocomposites and its morphological, mechanical, thermal and rheological properties. *Compos. Part B Eng.* **184**, 107717 (2020)
11. D. Krapež Tomec, M. Schöflinger, J. Leßlhuber, U. Gradišar Centa, J. Žigon, and M. Kariž, The Effects of Microcrystalline Cellulose Addition on the Properties of Wood–PLA Filaments for 3D Printing. *Polymers* **16**, 836 (2024)
12. A. E. Engelbrecht-Wiggans and A. L. Forster, Analysis of strain correction procedures for single fiber tensile testing. *Compos. Part Appl. Sci. Manuf.* **167**, 107411 (2023). [doi: 10.1016/j.compositesa.2022.107411](https://doi.org/10.1016/j.compositesa.2022.107411)
13. C. M. González-Henríquez, F. E. Rodríguez-Umanzor, M. A. Sarabia-Vallejos, and J. Rodríguez-Hernández, 4D Printing Using Multifunctional Polymeric Materials: A Review. *Encyclopedia of Materials: Plastics and Polymers*. 17–36 (2022)
14. I. Plamadiala, C. Croitoru, M. A. Pop, and I. C. Roata, Enhancing Poly(lactic acid) (PLA) Performance: A Review of Additives in Fused Deposition Modelling (FDM) Filaments. *Polymers* **17**, 191 (2025) [doi: 10.3390/polym17020191](https://doi.org/10.3390/polym17020191)